A NUMERICAL MODEL FOR DUNE DYNAMICS

by J. Sündermann, Prof. Dr. rer. nat., Institut für Meereskunde, Universität Hamburg

H.-J. Vollmers, Prof. Dr.-Ing., Lehrstuhl für konstruktiven Wasserbau, Hochschule der Bundeswehr München

W. Puls, Dipl.-Phys., Sonderforschungsbereich 79, Technische Universität Hannover

Summary

A numerical sediment transport model is formulated that serves especially for the simulation of bedform mechanics. The model is based on the idea that sediment transport is determined by the erosion rate and the path length of bed material. Formulas for the erosion rate and the path length are derived from physical considerations and from measurements; they depend mainly on the local values of the shear velocity and the mean flow velocity near the bed. The behaviour of detached sediment is simulated by a Monte Carlo procedure, which is based on the mean flow velocities and the eddy viscosity. All flow properties that are needed for the sediment transport model are computed by a numerical flow model that includes two turbulence equations. Results of the flow model and the sediment transport model are compared with measured data.

NOTATION

A	eddy viscosity	$[cm^2\ s^{-1}]$
D	mean grain diameter	$[cm]$
g	acceleration of gravity	$[cm\ s^{-2}]$
h	bed height	$[cm]$
H	mean water depth	$[cm]$
k	$= 0,5\ (\overline{u'^2} + \overline{v'^2} + \overline{w'^2})$, turbulent kinetic energy (per unit mass)	$[cm^2\ s^{-2}]$
p	pressure	$[g\ cm^{-1}\ s^{-2}]$
q_s	sediment transport rate	$[cm^3\ cm^{-1}\ s^{-1}]$
u, w	local mean flow velocities in x- and z-direction	$[cm\ s^{-1}]$
u', v', w'	turbulent flow fluctuations in x-, y- and z-direction	$[cm\ s^{-1}]$
u_{bed}, w_{bed}	mean flow velocities 1 cm above the bed	$[cm\ s^{-1}]$
u_m	mean (depth integrated) flow velocity	$[cm\ s^{-1}]$
$-\overline{u'\ w'}$	Reynolds shear stress	$[cm^2\ s^{-2}]$
$v_*^{cr,e}$	critical shear velocity for the end of grain movement	$[cm\ s^{-1}]$

v_*	effective shear velocity	$[cm\ s^{-1}]$
v_*^k	shear velocity calculated from k	$[cm\ s^{-1}]$
v_*^{cr}	critical shear velocity for material entrainment	$[cm\ s^{-1}]$
x	horizontal coordinate in flow direction	[cm]
y	lateral horizontal coordinate	[cm]
z	vertical coordinate	[cm]
η	erosion rate of sediment	$[cm^3\ cm^{-2}\ s^{-1}]$
σ	path length of moving grains	[cm]

1 INTRODUCTION

Ripples and dunes develop in the lower regime of alluvial flows. Dunes are large-scaled bed structures which can have a height of about 0.25 of the water depth and which influence appreciably the transport of bed material.

Experimental research about bedforms has achieved a good deal of progress; most efforts were directed to laboratory experiments. On the other hand, theoretical knowledge about bedforms is meager. One reason for the lack of knowledge on this field is the complexity of the interdependencies between flow, sediment transport and bed deformation. An important point among this set of problems is the impact of turbulent flow fluctuations on the bed material.

2 FLOW COMPUTATION

We only consider two-dimensional (horizontal (x) - vertical (z)) flows. The flow model uses the Reynolds equations and the continuity equation in order to compute the pressure p and the mean flow velocities u and w (see Sündermann and Puls /1/), and it uses the equations derived by Launder and Spalding /2/ to compute the turbulent kinetic energy k and its dissipation rate ε. From k and ε we obtain the eddy viscosity A.

The flow equations are solved by a finite difference procedure. We only compute stationary flows. The flow model is the basis for the calculation of sediment transport. Therefore we must take care that especially the near bed flow is simulated as well as possible. Fig. 1 gives an idea of the grid being used both for the computation of the flow and the sediment transport.

Fig. 4 shows a comparison of measured and calculated flow quantities. It must be emphasized that discrepancies are not only caused by the shortcomings of the flow model, but also by shortcomings of the measurements (which is especially valid for turbulence measurements). But we don't want to find excuses if the measured and the computed data do not coincide: in some respects the model is really imperfect. This is especially valid for the simulation of large-scale turbulence structures. In addition, problems arise due to the numerical solution procedure: the transformation of differential terms of the flow equations into finite difference terms always causes a loss of physical information.

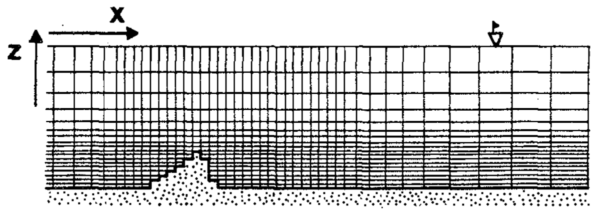

Fig. 1 : Computational Grid

The comparison of measured and computed data is performed by means of two flow examples: a flow above a negative step (Fig. 2) and a flow above a schematized dune (or to be more precise, a range of dunes, Fig. 3).

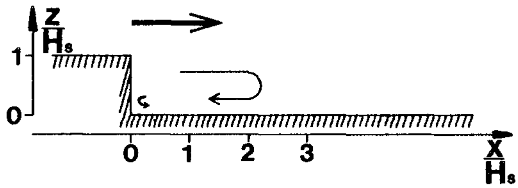

Fig. 2 : Negative Step Geometry

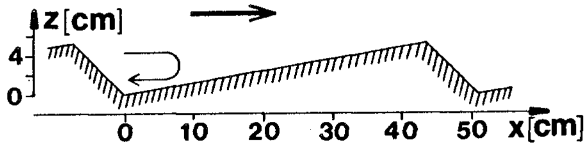

Fig. 3 : Dune Geometry

The experiment with the negative step was performed in a wind tunnel by Moss et al. /3/. The height of the wind tunnel is 84 cm, the step height H_s is 7.6 cm, the mean air velocity is about u_m = 1000 cm s^{-1}, the kinematic viscosity is 15 $cm^2 s^{-1}$. Fig. 4 shows vertical profiles

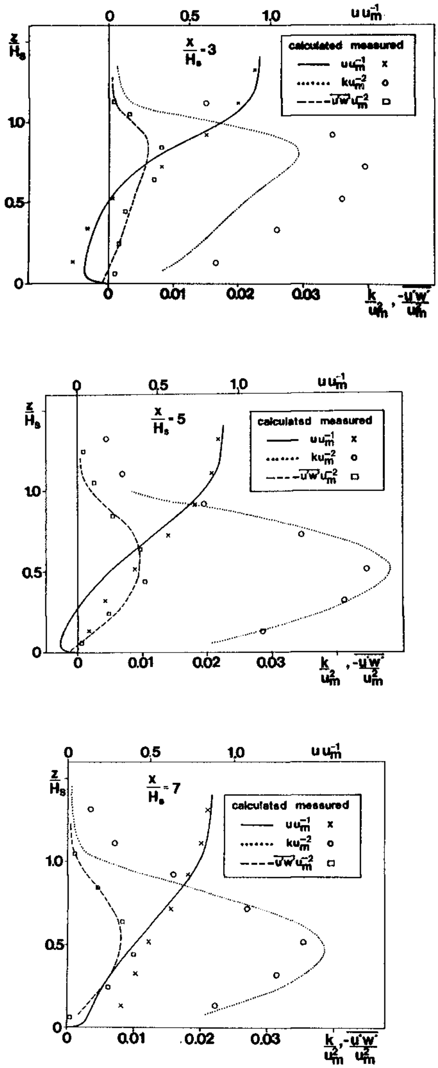

Fig. 4 : Vertical profiles of u, k and $-\overline{u'w'}$; flow above a negative step, data from Moss et al. /3/

of measured and calculated values of the mean horizontal velocity u, the shear stress $-\overline{u'w'}$ (which is expressed in the model by $A \frac{\partial u}{\partial z}$) and the turbulent kinetic energy at the positions $x H_s^{-1} = 3, 5$ and 7 (compare Fig. 2). The length of the separation zone in the lee of the step is calculated to be 5.7 H_s, while the measured value is 5 H_s. This can be seen in Fig. 4 by the disagreement of measured and calculated u at $x H_s^{-1} = 5$ and 7. Fig. 5 shows a comparison of the measured and the computed bottom pressure.

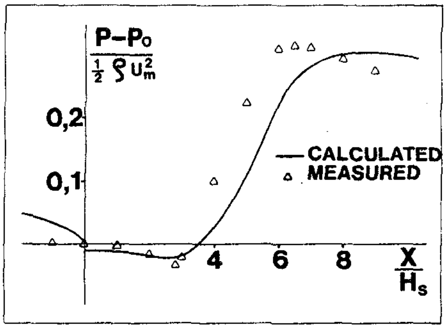

Fig. 5 : Bottom pressure; flow above a negative step, data from Moss et al. /3/

Rifai and Smith /4/ measured the water flow above dune-shaped bedforms in a flume. The water depth at x = o (see Fig. 3) is H_o = 30.5 cm, the mean flow velocity at x = o is 57.65 cm s^{-1}. The measured quantities are $\overline{u'^2}$ and u. For the comparison of k and $\overline{u'^2}$, we assume $\overline{v'^2} + \overline{w'^2} = \overline{u'^2}$. Fig. 6 shows the comparison of measured and calculated vertical profiles of u and k. As well as in the case of the negative step, the agreement is satisfactory. The greatest differences appear at x = 7.6 cm (see Fig. 3), where at $z H_o^{-1} \approx 0.15$, the measured k is much larger than the calculated k. The reattachment point was measured at x = 15 cm; the same result is given by the model.

In addition to the two bed examples shown above, the model was also applied to other bed configurations.

On the whole, the flow model of course would need some corrections. However, being compared with the flow conceptions that are used till today for tackling sediment transport, our flow model is a real improvement, both concerning the structure of the mean flow and the turbulence.

3 SEDIMENT TRANSPORT MODEL

3.1 Formulation of the model

The sediment transport model serves for the small-scale simulation of sediment transport. The computation is based on a division of the bed into horizontal intervals. For any of these intervals, the flow model

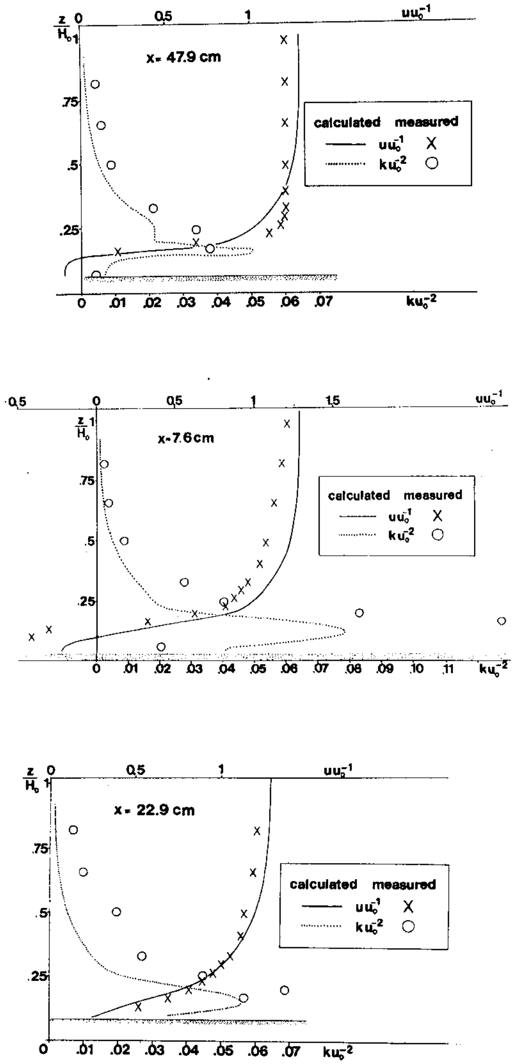

Fig. 6 : Vertical profiles of u and k; flow above dunes, data from Rifai and Smith /4/

yields the near bed values for u, w, k and A.

One of the main faults of earlier works on bedform mechanics is the direct relation between the flow forces (usually in the form of the shear velocity v_*) inducing the sediment transport and the rate of sediment transport q_s. That this is wrong is easily shown by a simple example. Imagine a plane bed with a flow running above it; v_* is constant all over the bed. The upstream part of the bed is rigid, the downstream part is movable. Of course, q_s is zero on the rigid bed and develops from zero to an asymptotic value on the movable bed. Thus q_s varies over the movable bed though v_* is constant. A similar situation is found on bedforms downflow of the reattachment point. Therefore, in order to investigate bedform mechanics, the assumption of a direct relationship between v_* and q_s must be dropped.

Our device for the calculation of sediment transport is expressed by

$$(1) \qquad \frac{\partial |q_s|(x)}{\partial x} + \frac{|q_s|(x)}{\sigma(x)} = \eta(x)$$

with σ being the path length a grain travels under homogeneous conditions from entrainment to deposition; η is the rate of material (measured by the total volume of bed material) being entrained from the bed per square unit and unit time. Equation (1) is valid for the absolute values of q_s only, because σ is positive definite. The sign of q_s is determined from the direction of the local mean flow near the bed. If η and σ are constant with respect to x, the differential term in (1) can be omitted, yielding

$$q_s = \eta \cdot \sigma$$

The next task is to get information about η and σ. There exist only a few experiments that have been concerned with direct measurements of η or σ. The erosion rate of non-consolidated mud was measured at HRS /5/. Takahashi, whose data is given by Nakagawa and Tsujimoto /6/, measured the probability of grains to be entrained on a flat bed. The information of both works can be expressed by ($v_* > v_*^{cr}$):

$$(2) \qquad \eta = const_\eta \cdot D \cdot \frac{v_*^2 - (v_*^{cr})^2}{(v_*^{cr})^2}$$

with $const_\eta = 0.018\ s^{-1}$ from Takahashi's data and $const_\eta \approx 0.05\ s^{-1}$ from the HRS-data.

The path length σ was measured by Wulzinger and Liebig /7/ and by Nakagawa and Tsujimoto /6/. The quintessence of these measurements is a formula for the grain path length of bed load (for $v_* > v_*^{cr,e}$)

$$(3) \qquad \sigma_{bed} = 820 \frac{\rho}{(\rho_s - \rho) g} \, |u_{bed}| \, (v_* - v_*^{cr,e})$$

The values for $v_*^{cr,e}$ are taken from the Hjulstroem diagram (in Graf /8/).

The path length of suspended load cannot be deduced from direct measurements. The behaviour of suspended material is controlled by the settling velocity w_s and the eddy viscosity A. Our formula reads (for a derivation see Puls /9/)

$$\sigma_{sus} = \sigma_{bed} \left(1 + c_s \frac{A^s \, v_*^A}{w_s^3}\right)$$

A^s is an eddy viscosity being representative for the near bed zone, v_*^A is a shear velocity that is determinded from A^s. c_s is a constant with the value $c_s = 30\ s^{-1}$.

The path length σ of total load (= suspended load + bed load) is determinded by

$$\frac{1}{\sigma} = \frac{R_{sb}}{1 + R_{sb}} \frac{1}{\sigma_{sus}} + \frac{1}{1 + R_{sb}} \frac{1}{\sigma_{bed}}$$

with R_{sb} being the ratio of suspended load and bed load. Using the data of Guy et al. /10/, a rough formula for R_{sb} is

$$R_{sb} = 5 \frac{e^{-w_s z_s (A^s)^{-1}}}{1 - e^{-w_s z_s (A^s)^{-1}}}$$

with $z_s = 0.5$ cm.

3.2 CALCULATION OF THE SHEAR VELOCITY

An essential point for calculating q_s is the choice of the shear velocity v_*. Because turbulence is the predominant factor for the capability of the flow to erode a grain and to prevent its deposition, v_* should be derived from the intensity of turbulence at the bed.

Using k_{bed} as the turbulent kinetic energy at the bed level, we obtain a shear velocity v_* from the equation

$$v_*^k = 0.51\ (k_{bed})^{0.5}$$

Using v_*^k instead of v_* in (2) and (3), however, there is usually too much erosion in the reattaching zone of bedforms. Better results are achieved with

$$v_* = 0.7\ v_*^k + 0.3 \cdot 0.07\ (u_{bed}^2 + w_{bed}^2)^{0.5} \qquad (4)$$

which uses the near bed mean flow velocities 1 cm above the bed. The weights 0.7 and 0.3 are found empirically in order to achieve acceptable agreement of the bed profile and the curve of q_s in Fig. 10.

3.3 BEHAVIOUR OF DETACHED SEDIMENT

The transport equation (1) is based on the assumption that σ is evaluated from v_* and u_{bed} being specific for the near bed region. This assumption is not fulfilled for particles being transported over a bedform's crest and which get caught in the separation zone in the lee of the bedform. In this case the particles are exposed to the local flow conditions which have nothing in common with the near bed values for the same x-coordinate. This is generally true if flow detachment occurs.

In such a case the transport of sediment is not calculated by (1) but by a Monte Carlo procedure (e.g. Maier - Reimer /11/). During this procedure, single (fictitions) particles are exposed to the direct influence of the local mean velocities and the local turbulence. The particles describe random walks like that plottet in Fig. 7.

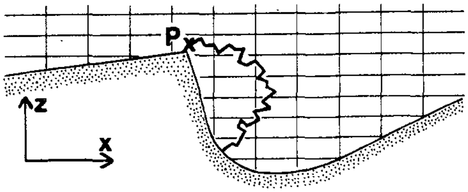

Fig. 7 : Random walk of a particle

The Monte Carlo procedure is tested by comparing its results with measurements of Allen /12/. Allen's experimental setup is shown in Fig. 8, simulating the lee slope of a bedform. Above the upper end of the slope,

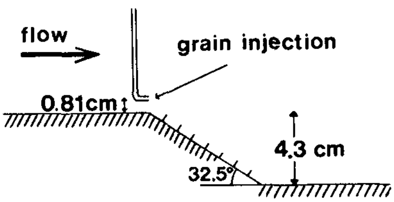

Fig. 8 : Experimental setup

sand grains are injected into the flow having a velocity u_g that equals that of the surrounding fluid. Touching the lee slope, the grains are arrested by a coat of glue. Measured and computed distributions of grains having settled down on the lee slope are shown in Fig. 9. On the

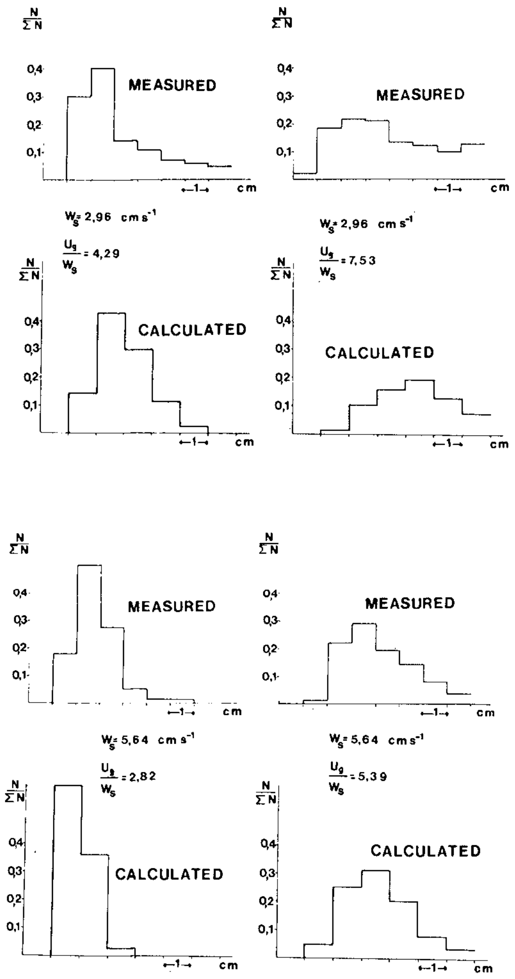

Fig. 9 : Distribution of settled particles

whole, the agreement is satisfactory; the centres of mass as well as the width of the distributions are reproduced quite well by the model.

4 SEDIMENT TRANSPORT OVER BEDFORMS

The transport model outlined above is applied to bedforms in unidirectional flow. For a bedform migrating with the velocity U_w without bed deformation, the relation

$$\frac{\partial q_s}{\partial x} = U_w \frac{\partial h}{\partial x} \tag{5}$$

is valid. The integration of (5) yields qualitatively

$$q_s(x) - q_{s,min} \sim h(x) - h_{min} \tag{6}$$

with $q_{s,min}$ and h_{min} being the minimum values of q_s an h respectively. The relation (6) fulfills the condition $q_s = q_{s,min}$ at $h = h_{min}$.

For our comparison we consider three widely different bedforms: a laboratory ripple, a laboratory dune and a dune in the Elbe river. The Figures 10, 11 and 12 show the comparison of the measured bed profiles

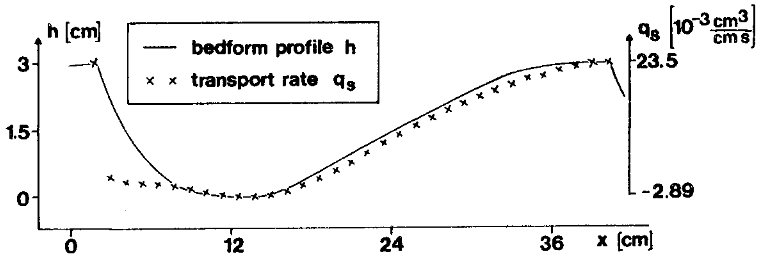

Fig. 10 : Comparison of h and q_s ; ripple profile taken from /13/, u_m = 30 cm s^{-1}, H = 13 cm, D = 0,042 cm

h (x) and the transport rates q_s (x) that are calculated by the transport model. The values of h_{min} and of $q_{s,min}$ are placed on the same level. Further, the scale of q_s is chosen in oder to obtain identical maxima for h and q_s. Thus if the relation (6) is really fulfilled, the curves of h and q_s must coincide irrespective whether U_w is simulated by the model or not. As we see from Figures 10, 11 and 12, the curves of q_s and h agree quite well. Of course, we must not forget that the model was drafted just in order to achieve the agreement of h and q_s. But nevertheless, we obtain the confirmation that our conception of sediment transport, i.e. the calculation of q_s with the help of η and σ, is able to yield good results.

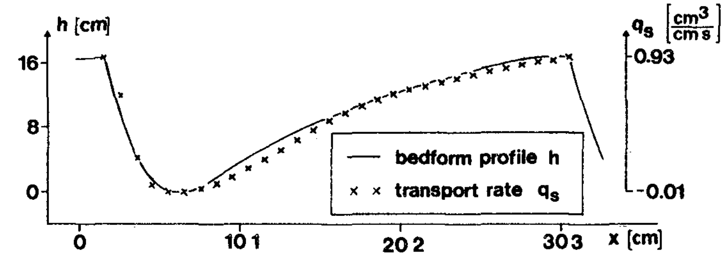

Fig. 11 : Comparison of h and q_s ; dune profile taken from /14/, u_m = 62 cm s^{-1} , H = 73 cm, D = 0.026 cm

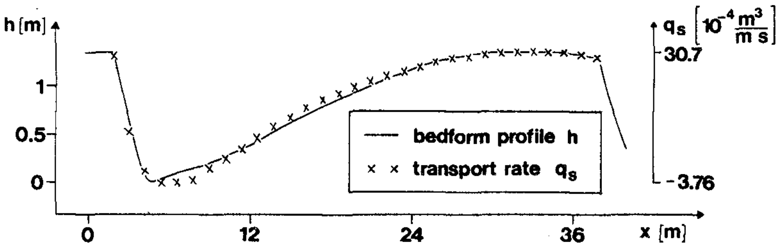

Fig. 12 : Comparison of h and q_s ; dune profile taken from /15/, u_m = 120 cm s^{-1} , H = 700 cm, D = 0.04 cm

As stated above, the agreement of h and q_s is qualitative only. An additional quantitative comparison means to compare the absolute values of measured and calculated q_s.

No data is available for the dune in the Elbe river.

The transport rate over the ripple was measured to be q_s = $6 \cdot 10^{-4}$ cm^{2}s^{-1} whereas the calculated value is $q_s = 8 \cdot 10^{-3}$ cm^2 s^{-1} (using const$_\eta$ = 0.036 s^{-1}). The discrepancy could be caused by a "firmness" of the skin of the laboratory sand ripple (see also Guy et al. /10/): because of the low transport rate, a moving grain has a good chance to find a refuge in the bed, where it can easily resist to further flow attacks. Such a bed firmness decreases the erosion rate η appreciably.

For the laboratory dune, the qualitative comparison yields a better result: the measured migration velocity of the dune is U_w= 0.049 cm s^{-1} , while the calculated value is $U_w = 0.045$ cm s^{-1} (with $const_\eta$ = 0.036 s^{-1}).

The computed values of v_*^k, v_*, u_{bed} and σ over the three bedforms are shown in Figures 13, 14 and 15. The curves of v_*^k always have their

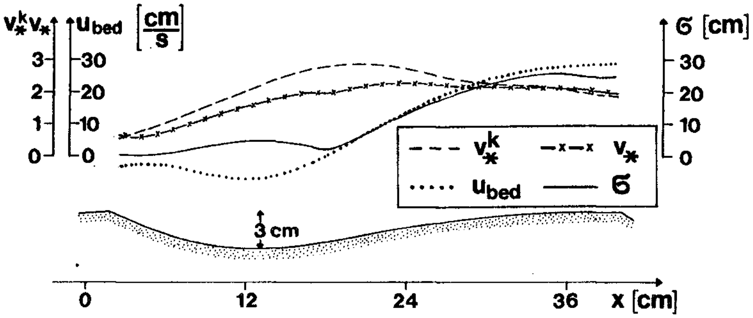

Fig. 13 : Computed values of v_*^k, v_*, u_{bed} and σ over the ripple taken from /13/

maximum in the reattaching zone. According to the influence of u_{bed} (see equation (4)), the curve of the effective shear velocity v_* is more smooth than that of v_*^k . The values of u_{bed} are negative in the recirculation zones. The most important point in Figures 13, 14 and 15 is the fact that σ is always in the order of the bedform length.

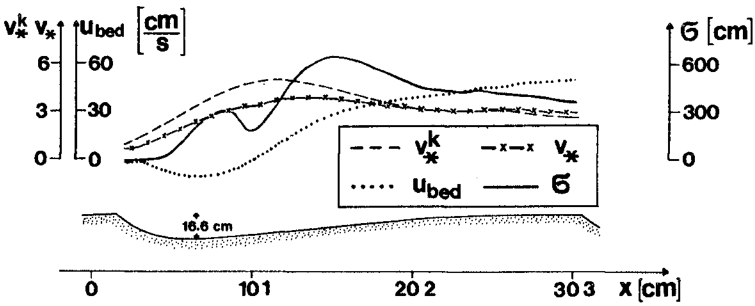

Fig. 14 : Computed values of v_*^k, v_*, u_{bed} and σ over the dune taken from /14/

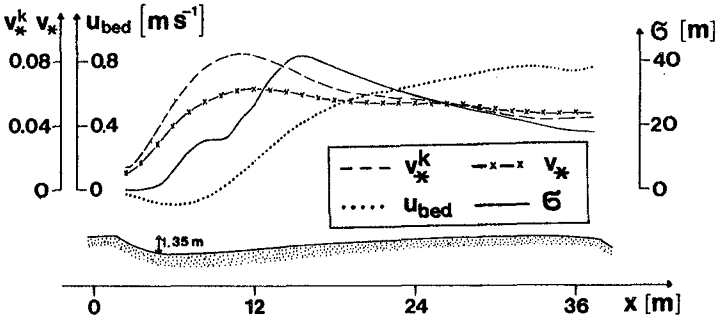

Fig. 15 : Computed values of v_*^k, v_*, u_{bed} and σ over the dune taken from /15/

CONCLUSION

Up to now, theoretical attempts to simulate in detail the sediment transport over bedforms and to explain the characteristics of bedforms have suffered from the following shortcomings:

- the flow was simulated in a simplified way only (e.g by using potential flow theory)
- turbulence was not included in the considerations
- a direct relationship between the flow parameters and the transport rate was assumed

The numerical model outlined in this paper avoids these shortcomings and is thus able to simulate in a physically adequate way the sediment transport over bedforms.

ACKNOWLEDGEMENT

The work reported in this paper was performed within the investigation program of the Sonderforschungsbereich 79, Hannover.

REFERENCES

/1/ SÜNDERMANN, J. and PULS, W. (1980) Numerical modelling of sediment transport in coastal waters, in: Mathematical modelling of estuarine physics, Lecture notes on coastal and estuarine studies, editors: J. Sündermann and K.-P. Holz, Springer

/2/ LAUNDER, B.E. and SPALDING, D.B. (1972) Mathematical models of turbulence, Academic Press, London.

/3/ MOSS, W.D., BAKER , S. and BRADBURY, L.J.S. (1977) Measurements of mean velocity and Reynolds stress in some regions of recirculating flow, Symposium on turbulent shear flows, University Park, Pennsylvania, Vol. 1, 13 A

/4/ RIFAI, M.F and SMITH, K.H.V. (1971) Flow over triangular elements simulating dunes, J. of the Hydr. Division, Proceedings of the ASCE, HY 7

/5/ HRS (1977) Properties of Grangemouth mud, Report No. EX 781

/6/ NAKAGAWA, H. and TSUJIMOTO, T. (1977) On probabilistic characteristics of motion of individual sediment particles on stream beds, in: Hydraulic problems solved by stochastic methods, editors: P. Hjorth, L. Joensson, P. Larsen, Proceeding, IAHR

/7/ WULZINGER, W. and LIEBIG, W. (1979) Private communication

/8/ GRAF, H.W. (1971) Hydraulics of sediment transport, McGraw-Hill Book Company

/9/ PULS, W. (1980) Numerical simulation of bedform mechanics, Thesis (Ph. D.), University of Hamburg, to appear

/10/ GUY, H.P., SIMONS, D.B. and RICHARDSON, E. V. (1966). Summary of alluvial channel data from flume experiments, Geologic Survey Professional Paper 462 - I

/11/ MAIER - REIMER, E. (1980) On the formation of salt wedges in estuaries, Mathematical modelling of estuarine physics, edited by J. Sündermann and K.-P. Holz, Springer

/12/ ALLEN, J.R.L. (1968) Current Ripples, North Holland Publishing Company, Amsterdam

/13/ RAUDKIVI, A.J. (1963) Study of sediment ripple formation, J. of the Hydr. Division, Proceedings of the ASCE, HY 6

/14/ BODE, E. and ZANKE, U. (1977) Private communication

/15/ STEHR, E. (1975) Grenzschicht - theoretische Studie über die Gesetze der Strombank- und Riffelbildung, Hamburger Küstenforschung, Heft 34